Procedia Computer Science

Volume 80, 2016, Pages 1601–1611

ICCS 2016. The International Conference on Computational Science

A New Approach to Ocean Eddy Detection, Tracking, and Event Visualization

–Application to the Northwest Pacific Ocean–

Daisuke Matsuoka[1], Fumiaki Araki[1], Yumi Inoue[1], and Hideharu Sasaki[1]

Japan Agency for Marine-Earth Science and Technology (JAMSTEC), Yokohama, Japan
{daisuke,arakif,inouey,sasaki}@jamstec.go.jp

Abstract

High-resolution ocean general circulation models have advanced the numerical study of ocean eddies. To gain an understanding of ocean eddies from the large volume of data produced by simulations, visualizing just the distribution of eddies at each time step is insufficient; time-variations in eddy events and phenomena must also be considered. However, existing methods cannot accurately detect and track eddy events such as amalgamation and bifurcation. In this study, we propose a new approach for eddy detection, tracking, and event visualization based on an eddy classification system. The proposed method detects streams and currents in addition to eddies, and it classifies detected eddies into several categories using the additional stream and current information. By tracking how the classified eddies vary over time, it is possible to detect events such as eddy amalgamation and bifurcation as well as the interaction between eddies and ocean currents. We visualize the detected eddies and events in a time series of images (or animation), enabling us to gain an intuitive understanding of a region of interest hidden in a high-resolution data set.

Keywords: Ocean eddy, ocean general circulation model, feature extraction and tracking, visualization

1 Introduction

Ocean eddies play an important role in transferring heat, energy, and material in the ocean. They also affect global ocean dynamics, weather conditions, and commercial activities such as fisheries [8]. Understanding ocean eddies has implications for both human activities and ocean sciences, and satellite observational data have been used in many ocean eddy studies [18, 10]. Recent advances in supercomputing technology have also allowed the development of Ocean General Circulation Models (OGCMs) for investigating global ocean dynamics [5, 15]. Sasaki et al. succeeded in using a high-resolution OGCM to reproduce mesoscale ($\mathcal{O}$(100 km)) and submesoscale ($\mathcal{O}$(10 km)) eddies and to reveal their global and seasonal variability [14]. Such high-resolution numerical studies have advanced our understanding of eddies, but issues such

Selection and peer-review under responsibility of the Scientific Programme Committee of ICCS 2016

doi:10.1016/j.procs.2016.05.491

as eddy generation mechanisms, statistical properties, and influences on fishery remain to be explored.

Data visualization is an indispensable technique for helping scientists understand the meaning of numerical simulation results. This is especially true for data sets generated by high-resolution OGCMs, which reproduce such a vast number of eddies that it is difficult to use traditional visualization methods to address "when, where, [and] what kind of phenomena have occurred" [20, 13, 21, 7]. Visualizing events such as eddy creation, dissipation, amalgamation, and bifurcation in addition to visualizing position information makes it possible to more intuitively understand eddy behavior. In order to visualize all these events, it is first necessary to detect eddies and track how they change over time.

A number of eddy detection methods have been proposed in the field of physical oceanography (e.g. [17, 9, 19, 3, 12]). These methods can identify the core regions and center points of eddies, however, the outer boundary is not precisely determined during eddy interaction events such as amalgamation and bifurcation (will be described in detail in 3.1). Thus, most eddy tracking methods based on these techniques [2, 4] cannot detect eddy amalgamation and bifurcation events; these technique also cannot automatically detect interactions between eddies and ocean currents. The visualization research community has published a number of studies about feature tracking, event detection, and visualization [16, 11]; the application of these studies to ocean eddies has not previously been explored.

In this study, we propose a new method for eddy detection, tracking, and event detection that is able to treat eddy amalgamation, bifurcation, and interactions with ocean currents. Furthermore, we show how eddies and eddy events can be visualized to yield an intuitive understanding of the timing, location, and types of eddy events occurring. The manuscript is organized as follows. In section 2, we present the ocean simulation data used for this study. In section 3, we describe the conceptual framework and methods for our approach to eddy detection, tracking, and event detection. In section 4, we demonstrate our proposed visualization method. Finally, a summary of this work is provided in section 5.

2 Data set

The ocean simulation data used in this study is produced by the OGCM for the Earth Simulator (OFES) [5]. The OFES uses a finite difference method to solve the Navier-Stokes equations, the equation of continuity, the advection-diffusion equation, and the sea water equation of state to determine the time variation of velocity fields, density, pressure, temperature, and salinity in the ocean. The original version of OFES is a quasi-global model (it excludes the north and south polar regions) with a horizontal resulution of $1/10°$. We performed the northwest Pacific model of OFES [15] with $1/30°$ horizontal resolution in order to more accurately resolve mesoscale eddies. The entire simulation domain for this model is shown in Figure 1(a), which depicts the simulated relative vorticity; the analysis domain of this work is indicated by the black dashed rectangle within this panel. Panels (b), (c), and (d) in Figure 1 depict the simulated current speed (velocity magnitude), sea surface height (SSH), and the Okubo-Weiss parameter, respectively, within the analysis domain. The Okubo-Weiss parameter W is calculated by velocity field (u, v) and is defined as

$$W = s_n^2 + s_s^2 - \omega^2, \tag{1}$$

where $s_n = \partial u/\partial x - \partial v/\partial y$ and $s_s = \partial v/\partial x + \partial u/\partial y$ are the normal and shear components of strain, and $\omega = \partial v/\partial x - \partial u/\partial y$ is the relative vorticity.

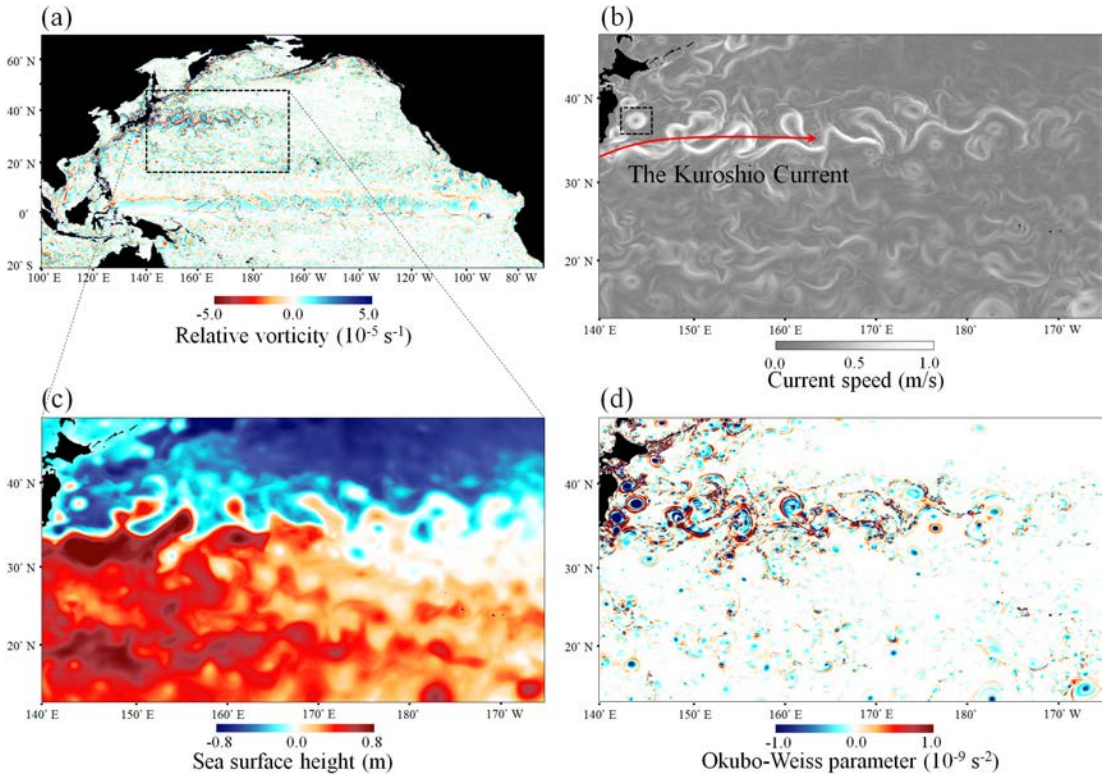

Figure 1: Ocean simulation data for January 1, 2001. Panel (a) shows the relative vorticity for the entire simulation domain (the analysis domain is indicated by the dashed black rectangle). The remaining panels show only the analysis domain and display: (b) current speed (magnitude of the velocity), (c) sea surface height (SSH), and (d) the Okubo-Weiss parameter.

Note that these variables are shown in just two dimensions; this is not intended to be a study of the three-dimensional configuration of eddies and currents. The simulation reproduces a large number of eddies in the vicinity of the Kuroshio Current, a strong ocean current indicated by the red solid line in Figure 1(b), which is why we selected this region for our analysis domain.

3 Methods

3.1 Basic Conceptual Framework

Ocean eddies are streams of water rotating around a central point; they are classified as either warm or cold depending on their temperature relative to the surrounding water. An example warm eddy is indicated by the black dashed box in Figure 1(b), with typical physical properties shown in Figure 2. Panels (a), (b), (c) and (d) in Figure 2 depict the velocity field, SSH, current speed, and the Okubo-Weiss parameter, respectively. The right side of panels (b), (c) and (d) shows how these variables vary across the eddy. In the Northern Hemisphere, warm eddies flow clockwise and display an upward convex structure, whereas cold eddies flow counterclockwise with a downward convex structure; these rotation directions are reversed in

the Southern Hemisphere.

The center of a warm eddy can be easily detected because it is a critical point in the velocity field, a local maximum in the SSH, and a local minimum in the Okubo-Weiss parameter. Accurately identifying an eddy's outer boundary is not as easy. Intuitively, the outer boundary of the eddy in Figure 2(a) is indicated by a red dashed oval (the boundary between fast flow region of eddy and the surrounding area), and the location of the peak current speed is indicated by the yellow dashed oval in Figure 2(a).

Previous studies have used two types of eddy boundary detection methods: threshold-based and geometry-based. The most widely used threshold-based method uses the Okubo-Weiss parameter, which compares relative vorticity to strain; a negative value of the Okubo-Weiss parameter indicates that relative vorticity dominates over strain, which tends to be true in the inner part of an eddy [9, 19]. For our example eddy, this method places the eddy boundary inside the yellow dashed line in Figure 2; the detected eddy is thus considerably smaller than the actual eddy (red dashed line). Geometry-based boundary detection methods use contour lines in SSH, defining the eddy's outer boundary to be the outermost closed contour surrounding the center point of the eddy [3]. However, this method breaks down during certain eddy events. For example, during an amalgamation event, the close proximity of two detected eddies causes the outermost closed contour lines to underestimate the size of the eddies, as shown in Figure 3(a). This limitation is similar to that of the winding angle method [12] which detects the largest semi-closed streamline within a vector field. The many other eddy detection methods [1, 22] based on the above techniques suffer from similar problems.

In order to accurately detect and track eddies during amalgamation and bifurcation events, we separate the detection of an eddy's inner and outer regions in this study. This approach is based on the fact that the interior of an eddy has a convex shape and is surrounded by a fast flowing outer region. The inner region of an eddy will have a negative Okubo-Weiss parameter, so we define the boundary of the upward or downward convex inner region including a eddy's center point with the negative Okubo-Weiss parameter. To define the boundary for the eddy's outer, fast flowing region, we use a current speed threshold parameter. Our approach then uses the combined inner and outer regions to define the eddy, as shown in Figure 3(b); during the amalgamation event shown in the figure, the outer boundaries determined from the fast flow region correspond well to the actual eddy boundaries.

3.2 Eddy Detection

The first step in eddy detection is to identify the center point of each eddy from SSH and velocity field data. Local maxima and minima in SSH are detected using a 9×9 grid filter, shown in Figure 4(a); although the hybrid detection method [22] uses a 5×5 grid filter, the size of our filter is determined by the target eddy size (eddies larger than 30 km for this study). These filters detect the local maxima and minima points from which SSH value decreases (for warm eddy) or increases (for cold eddy) toward the outside eight direction as shown in Figure 4 (a). Some local maxima and minima occur outside of eddies, so only points with negative values of the Okubo-Weiss parameter are considered to be eddy center points; this is consistent with the hybrid detection method [22]. The resulting warm and cold eddy center points are indicated by red and blue points in Figure 4(b), respectively.

Next, the inner regions of the eddies are detected using SSH contour lines; the outermost closed contour line defines an eddy's inner region boundary using a SSH threshold parameter. Scanning the value of a inflextion point of SSH from the eddy's center point toward the outside during the entire 360 degree, the highest SSH value on the inflextion points is determined as the

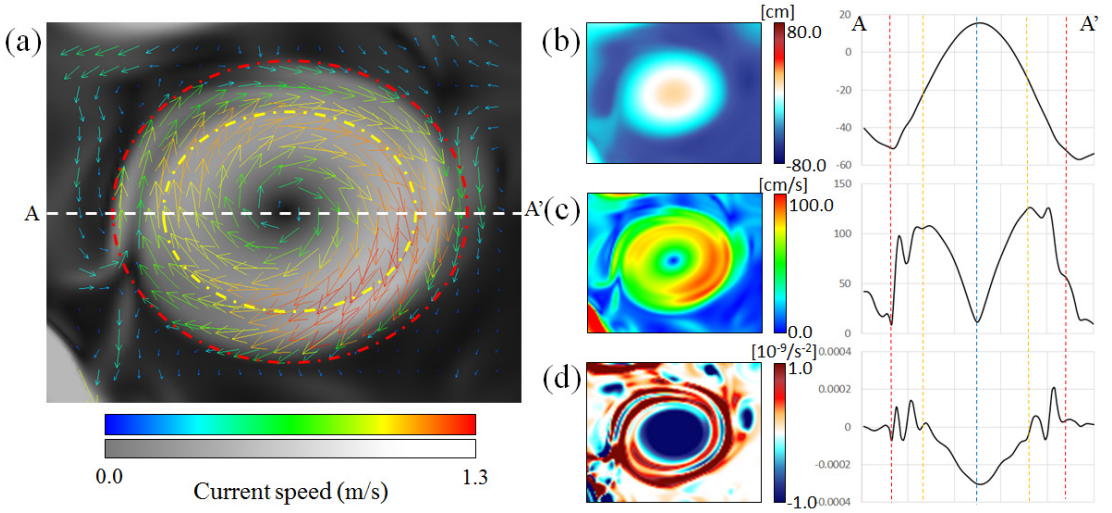

Figure 2: Example physical properties of a warm eddy: (a) velocity field, (b) sea surface height (SSH), (c) current speed, and (d) Okubo-Weiss parameter. The red dashed oval in panel (a) represents the eddy's outer boundary, while the yellow dashed oval indicates the location of the peak current speed. The right-hand plots in panels (b), (c), and (d) are traces along the line A-A', the white dashed line in panel (a), for each physical property.

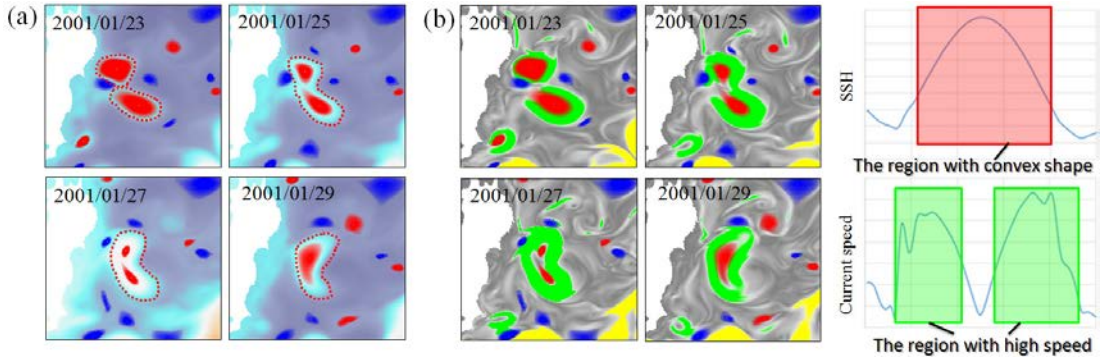

Figure 3: Detection of eddies during an amalgamation event using (a) an SSH-based method and (b) our method. In panel (a), the red area indicates the eddy detected by the SSH contour, and the red dashed line indicates the actual eddy boundary (intuitively extracted by the authors). In panel (b), the red area indicates the inner eddy region and the green area indicates the fast flowing, outer eddy region.

threshold value for inner region boundary. We then want to detect streams by finding areas of fast flow relative to the local current speed. For our analysis, we use a current speed threshold of 0.6 m/s in order to investigate eddies in the vicinity of the Kuroshio Current (which has a typical speed of over 0.6 m/s). The resulting detected eddies and streams are depicted in Figure 4(c); red, blue, and green regions indicate warm eddies, cold eddies, and stream regions, respectively. Streams of especially large size (here, their horizontal area are 50,000km^2 and

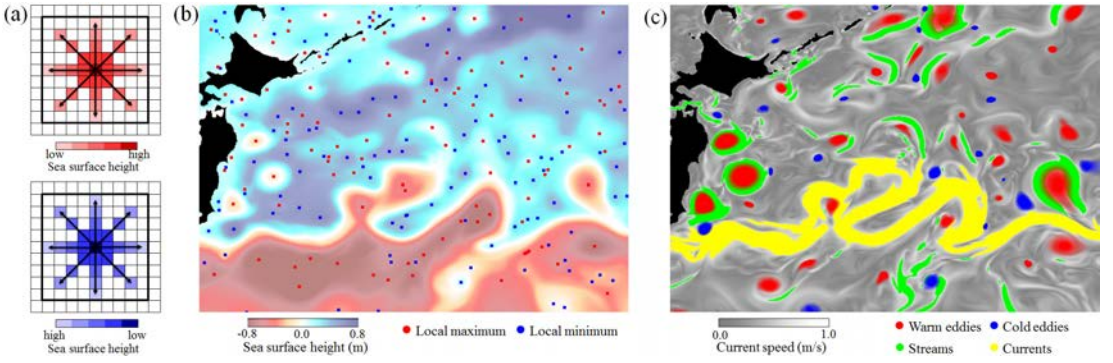

Figure 4: Eddy detection sequence: (a) filter for detecting warm eddy centers (top) and cold eddy centers (bottom), (b) identified eddy centers with negative Okubo-Weiss parameters (red indicates a warm eddy, blue indicates a cold eddy), and (c) detected warm eddies, cold eddies, streams, and currents.

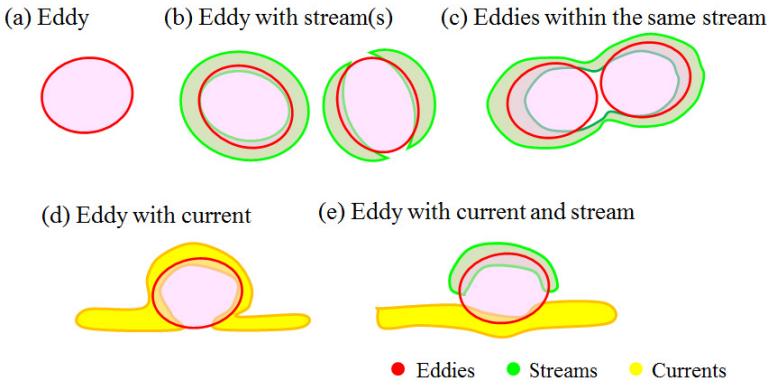

Figure 5: Eddy classification system: (a) eddy, (b) eddy with streams(s), (c) eddies within the same stream, (d) eddy with current, and (e) eddy with current and stream.

over) are defined as current regions and are shown in yellow.

Based on how they relate to streams or currents, the detected eddies are classified into the following five types: (a) eddy, (b) eddy with stream(s), (c) eddies within the same stream, (d) eddy with current, and (e) eddy with current and stream. These five types are illustrated in Figure 5. Types (a) and (b) are distinguished by the presence or absence of a stream region. Type (c) eddies can be used to identify amalgamation and bifurcation events, and types (d) and (e) are used for detecting the interaction between eddies and ocean currents.

3.3 Eddy Tracking and Event Detection

Once eddies have been identified, the next step is to apply a feature tracking algorithm to detect variations in individual eddies and events over time. While several feature tracking methods have ever been proposed [2, 4], we adopt the overlapping method because it is easy to implement and has a low computational cost [16]. The use of the overlapping method for five types of eddies (simplified to one-dimension rather than two) is shown in Figure 6 and described below.

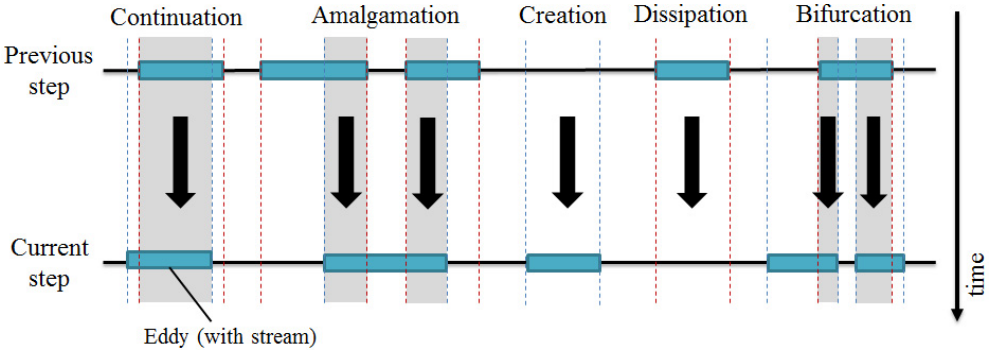

Figure 6: A conceptual representation of eddy tracking using the overlapping method in one-dimension for five types of eddy events.

This method automatically correlates eddies between the previous and current time steps using their spatial overlap as follows:

- `continuation` – An eddy from the previous time step corresponds to just one eddy in the current time step (no interaction with other eddies).
- `amalgamation (or merge)` – Two eddies from the previous time step correspond to one eddy in the current time step.
- `creation (or birth)` – An eddy in the current time step does not correspond to any eddies in previous time step.
- `dissipation (or death)` – An eddy from previous time step does not correspond to any eddies in the current time step.
- `bifurcation (or split)` – An eddy from the previous time step corresponds to two eddies in the current time step.

This method cannot be applied to data sets with coarse temporal resolution because identical features in previous and current step will not spatially overlap. However, our data has a 1 day time step, and eddies move at most 10 km over 1 day; this movement is much smaller than the eddy size we consider (30 km and larger), therefore we can assume that eddies will always spatially overlap between time steps.

We use the eddy feature tracking described above along with our eddy classification system (Figure 5) to track the evolution of eddies over time and identify eddy events. For example, by identifying "eddies within the same stream" (shown in Figure 5(c)), eddies undergoing amalgamation and bifurcation events can be detected. Feature tracking then allows us to identify the individual eddies from before and after these events, shown in Figures 7(a) and (b), demonstrating that this type of eddy is an intermediate stage. In the same way, the "eddy with current and stream" (Figure 5(d)) and the "eddy with current" (Figure 5(e)) classifications represent times when the ocean current has temporarily trapped an eddy during an interaction; Figures 7(c) and (d) show these two types of eddies joining and separating from the ocean current.

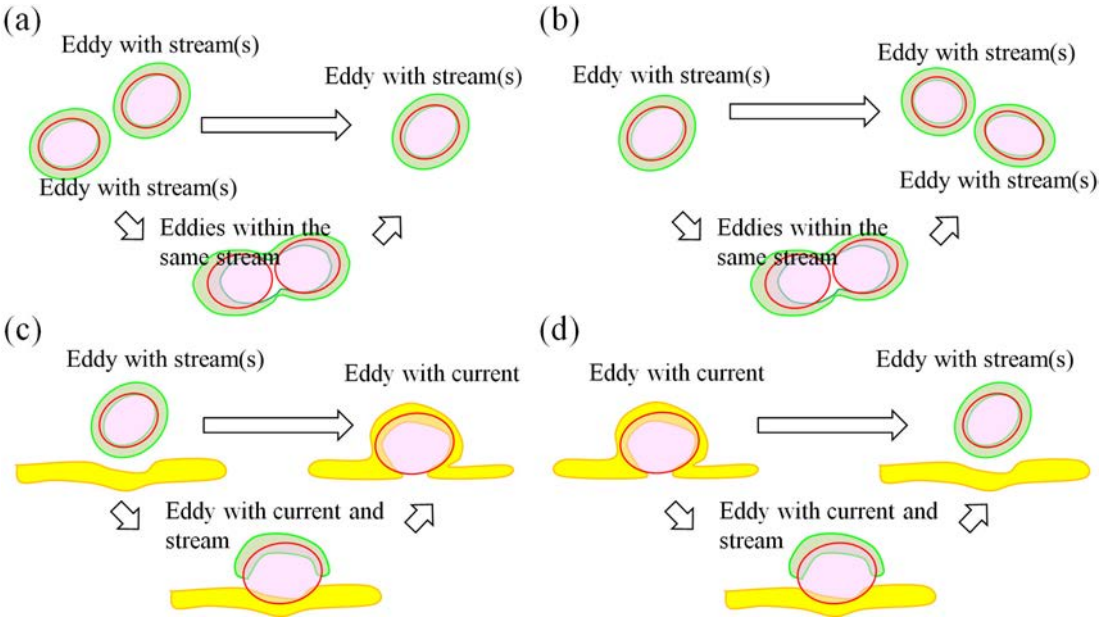

Figure 7: Event detection based on eddy tracking and classification: (a) amalgamation, (b) bifurcation, (c) merge to current and (d) separation from current.

4 Results

Numerical simulation results generated by high-resolution OGCMs reproduce such a large number and wide variety of eddies that it becomes difficult to use traditional visualization methods to identify interesting phenomena. In this study, we have proposed a method for eddy detection, tracking, and event detection that can be used to produce visualization images to help researchers intuitively understand the region of interest.

Our visualization technique uses different colors and brightness levels to indicate different phenomena; this approach is commonly utilized in ocean sciences [6]. Static warm eddies, cold eddies, streams, and currents (those with no events occurring) are colored by slightly dimmed (brightness = 50%) red, blue, green and yellow pixels, respectively. Bright colors (brightness = 100%) indicate eddies (and the stream regions around them) during events where no dissipation occurs, such as splitting or merging with each other or the ocean currents. Eddies that have dissipated since the previous time step are depicted in dark colors (brightness = 10%) in the current time step.

Figure 8 shows such a visualization for the amalgamation of two eddies. Two separate stream regions around two independent eddies merge into one stream around two separate eddy centers, and then the two eddies merge completely. The eddies and streams during and after the amalgamation event are highlighted using bright colors while the rest of the region remains dark. This visualization of the region during eddy amalgamation and bifurcation events makes it easier to intuitively understand the energy exchange occurring.

The separation of a warm eddy from the Kuroshio Current is visualized in Figure 9. The warm eddy is initially trapped within the Kuroshio Current, then it separates from the current, and finally it becomes an isolated warm eddy with a stream region; the warm eddy is represented by a bright red color at the time of its separation. This visualization shows how a warm eddy

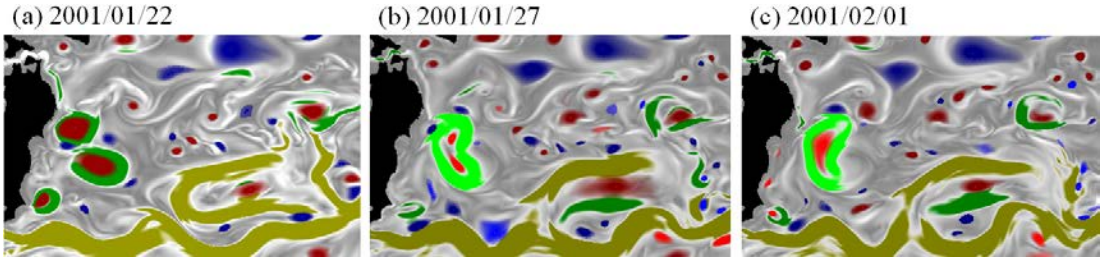

Figure 8: Visualization of an eddy amalgamation event over three time steps.

can penetrate from the south into the north area of the Kuroshio Current. When this happens, the Kuroshio Current is disconnected, as shown by the white dashed oval from July 30-31, 2001. Although we show only the sequential images here, we can combine similar images over long time periods to create a movie which very clearly shows the cold and warm water exchange in this ocean system by highlighting the interaction between ocean currents and eddies.

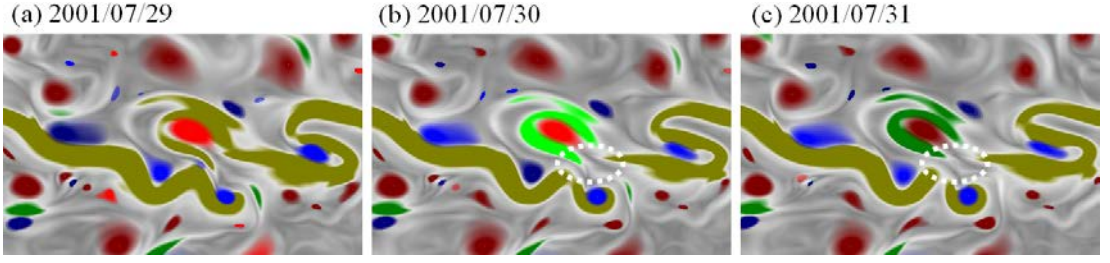

Figure 9: Visualization of a warm eddy's separation from the Kuroshio Current.

5 Summary and Discussion

We have proposed a new method of eddy detection, tracking, event detection, and visualization based on a hybrid definition of eddies using SSH, velocity fields, eddy classification, and feature tracking. We applied our method to high-resolution ocean simulation data, and we succeeded in identifying eddy events such as amalgamation, bifurcation, creation, continuation and dissipation. We also readily identify interactions between eddies and ocean currents, such as mergers and separations. Furthermore, we use highlighted colors to visualize regions of interest where eddy events occur to aid in forming an intuitive understanding of information-dense numerical simulation data.

In addition producing useful visualizations, our proposed method can also be used to produce and store data about eddies and eddy events. These results can be provided in an easily searchable database so oceanographers can identify eddies with specific properties and perform relevant statistical analyses. For example, an analysis of eddies including nutrient salt and ocean current with a school of fish could be used to investigate the relationship between eddies and fishery.

In this study, we used a current speed threshold value to extract streams and currents from the data, taking the typical speed of the Kuroshio Current into consideration. For this reason, our proposed method might not be immediately applicable to ocean areas other than

the northwest Pacific. In order to apply our proposed method to a global scale, it is necessary to improve our proposed method with regard to the current and stream detection.

Our proposed eddy detection and tracking method is a post processing approach applied after numerical simulations are run. Using this approach to track submesoscale structures at smaller temporal and spatial scales would require simulation data with very high temporal resolution; doing this in post processing is not realistic because it would require too much disk space for data storage. In the future, in-situ processing, where feature detection and tracking are carried out on a supercomputer during the numerical simulation, will likely be key to better understanding the mechanisms driving submesoscale ocean structures.

References

[1] F. J. Beron-Vera, Y. Wang, M. J. Olascoaga, G. J. Goni, and G. Haller. Objective detection of oceanic eddies and the agulhas leakage. *Journal of Physical Oceanography*, 43:1426–1438, 2013.

[2] D. B. Chelton, M. G. Schlax, R. M. Samelson, and R. A. Szoeke. Global observations of large oceanic eddies. *Geophysical Research Letters*, 34, 2007.

[3] F. Fang and R. Morrow. Evolution, movement and decay of warm-core leeuwin current eddies. *Deep-Sea Research II*, 50(12):2245–2261, 2003.

[4] E. Mason, A. Pascual, and J. C. McWilliams. A new sea surface height-based code for oceanic mesoscale eddy tracking. *Journal of Atmospheric and Oceanic Technology*, 32:1181–1426, 2014.

[5] Y. Masumoto, H. Sasaki, T. Kagimoto, N. Komori, A. Ishida, Y. Sasai, T. Miyama, T. Motoi, H. Mitsudera, K. Takahashi, H. Sakuma, and T. Yamagata. A fifty-year eddy-resolving simulation of the world ocean: Preliminary outcomes of ofes (ogcm for the earth simulator). *Journal of the Earth Simulator*, 1:35–56, 2004.

[6] D. Matsuoka, F. Araki, S. Kida, H. Sasaki, and B. Taguchi. Visualization for ocean general circulation model via multi-dimensional transfer function and multivariate analysis. *Transaction of the Japan Society for Simulation Technology*, 4(4):168–175, 2012.

[7] D. Matsuoka, F. Araki, and Y. Yamashita. Multiple scatter plots-based multi-dimensional transfer function and its application to ocean data visualization. *Journal of Advanced Simulation in Science and Engineering*, 2(2):292–308, 2015.

[8] J. C. McWilliams. The nature and consequence of oceanic eddies. *Eddy-Resolving Ocean Modeling, edited by M. Hecht and H. Hasumi, AGU Monograph*, pages 5–15, 2008.

[9] A. Okubo. Horizontal dispersion of floatable particles in the vicinity of velocity singularities such as convergences. *Deep Sea Research and Oceanographic Abstracts*, 17:445–454, 1970.

[10] A. Pascual, Y. Faugere, G. Larnicol, and P. Y. Le Traon. Improved description of the ocean mesoscale variability by combining four satellite altimeters. *Geophysical Research Letters*, 33(2), 2006.

[11] F. Reinders, F. H. Post, and H. J. W. Spoelder. Visualization of time-dependent data using feature tracking and event detection. *The Visual Computer*, 17:55–71, 2001.

[12] I. Ari Sadarjoen and F. H. Post. Detection, quantification, and tracking of vortices using streamline geometry. *Computers & Graphics*, 24(3):333–341, 2000.

[13] F. Samsel, M. Petersen, G. Abram, T. L. Turton, D. Rogers, and J. Ahrens. Visualization of ocean currents and eddies in a high-resolution global ocean-climate model. In *Proceedings of the International Conference on High Performance Computing, Networking, Storage and Analysis 2015*, November 2015.

[14] H. Sasaki, P. Klein, B. Qiu, and Y. Sasai. Impact of oceanic scale-interactions on the seasonal modulation of ocean dynamics by the atmosphere. *Nature Communications*, 5(5636), 2014.

[15] H. Sasaki, M. Nonaka, Y. Masumoto, Y. Sasai, H. Uehara, and H. Sakuma. An eddy-resolving hindcast simulation of the quasi-global ocean from 1950 to 2003 on the earth simulator. *High Resolution Numerical Modeling of the Atmosphere and Ocean*, pages 157–186, 2008.

[16] D. Silver and X. Wang. Volume tracking. In *Proceedings on IEEE Visualization '96*, October 1996.

[17] J. Villasenor and A. Vincent. An algorithm for space recognition and time tracking of vorticity tubes in turbulence. *CVGIP: Image Understanding*, 55(1):27–35, 1992.

[18] G. Wang, J. Su, and P. C. Chu. Mesoscale eddies in the south china sea observed with altimeter data. *Geophysical Research Letters*, 30(21), 2003.

[19] J. Weiss. The dynamics of enstrophy transfer in two-dimensional hydrodynamics. *Physica D*, 48:273–294, 1991.

[20] S. Williams, M. Petersen, P. T. Hecht, V. Pascucci, J. Ahrens, M. Hlawitschka, and B. Hamann. Adaptive extraction and quantification of geophysical vortices. *IEEE Transactions on Visualization and Computer Graphics*, 17(12), 2011.

[21] J. Woodring, M. Petersen, A. Schmeißer, J. Patchett, J. Ahrens, and H. Hagen. In situ eddy analysis in a high-resolution ocean climate model. *IEEE Transactions on Visualization and Computer Graphics*, 22(1):857–866, 2015.

[22] J. Yi, Y. Du, Z. He, and C. Zhou. Enhancing the accuracy of automatic eddy detection and the capability of recognizing the multi-core structures from maps of sea level anomaly. *Ocean Science*, 10:39–48, 2014.